Characterization and Catalytic Performance of Al-SBA-15 Catalyst Fabricated Using Ionic Liquids with High Aluminum Content

Obaid F. Aldosari * , Hassan Hassan , Mosaed S. Alhumaimess , Mohamed A. Betiha , Emad A. Ahmed , Laila M. Alhaidari , Afnan Altwala

Posted Date: 19 July 2023

doi: 10.20944/preprints202307.1258.v1

Keywords: Al-SBA-15; Mesoporous; ethylenediamine; trimethylamine; ionic liquid; Esterification reaction

Article

Characterization and Catalytic Performance of Al-SBA-15 Catalyst Fabricated Using Ionic Liquids with High Aluminum Content

Obaid F. Aldosari [1]*, Hassan M.A. Hassan [2], Mosaed S. Alhumaimess [2], Mohamed A. Betiha [3], Emad A.Ahmed [4], Laila M. Alhaidari [1] and Afnan Altwala [1]

[1] Department of Chemistry, College of Science, Majmaah University, Majmaah 11952, Saudi Arabia
[2] Department of Chemistry, College of Science, Jouf University, PO Box 2014, Sakaka, Saudi Arabia
[3] Egyption Petrolum Research Institute, Cairo 11727, Naser City, Egypt
[4] Department of Chemistry, Faculty of Science, Suez University, Suez, Egypt
* Correspondence: o.aldosari@mu.edu.sa

Abstract: This study involved the fabrication of a set of Aluminum ion-grafted SBA-15 utilizing ethylenediamine and trimethylamine ionic liquids. The primary objective was to examine the impact of the fabrication environment on the physicochemical characteristics of the catalysts. Comprehensive characterization of the Al-SBA-15 catalysts was conducted using various techniques, including XRD, FTIR, surface area, pyridine FTIR, 27Al-NMR, TGA, HRTEM, and FESEM, to analyze their physicochemical characteristics. Furthermore, the acidic characteristics were examined by conducting potentiometric titration in a nonaqueous solvent and employing FTIR spectroscopy to analyze the chemisorbed pyridine. The effectiveness of the fabricated acid materials was evaluated by testing their performance in the acetic acid esterification with butanol. The findings obtained reveal that the mesostructured of SBA-15 remains intact following the successful inclusion of Al3+ ions into the silica frameworks. Additionally, a remarkable enhancement in the existence of both Bronsted and Lewis acid centers is noted due to the grafting process of Al3+ ions. At temperatures of 80°C and 100°C, the reaction in Al-SBA-15(T-120) proceeds swiftly, reaching approximately 32% and 38% conversion, respectively, within a span of 110 minutes. The excellent catalytic performance observed in the esterification reaction can be attributed to two factors: the homogeneous distribution of Al3+ ions within the SBA-15 frameworks and the acidic character of Al-SBA-15. The findings further indicate that the grafting process for incorporating Al3+ ions into the silica matrix is more efficient.

Keywords: Al-SBA-15; mesoporous; ethylenediamine; trimethylamine; ionic liquid; esterification reaction

1. Introduction

The synthesis of mesoporous structure with large surface areas, homogeneous size distribution of pores and excellent chemical durability is currently a highly researched and relevant area, particularly due to its potential applications in metal ion separation, adsorption, and sensors [1]. Apart from these uses, mesoporous substances are viewed as a possible possibility for catalysis [2,3]. Acid-catalyzed processes are widely used in industry, particularly in oil refinement, petrochemical industry, and medication fabrication. Zeolites are broadly utilized as an acid catalyst, particularly in various industries [4]. Nevertheless, their microporous structure limits their applicability and makes them unsuitable for the handling of big organic compounds [5]. As a result, finding appropriate resources to address this problem is a top priority. In 1998, Stucky et al. developed an innovative classification system for mesoporous materials created under acidic conditions using neutral model. The produced material was named SBA-15 [6]. The hexagonally structured SBA-15 is mesoporous

 doi:10.20944/preprints202307.1258.v1

prearranged silica having talented characteristics as a catalyst support [7]. This due to its immense explicit surface area and adaptable porosity afford the mass transference and dispersion supremacy in the chemical processes enclose reactant, intermediate or product with radius higher than the zeolites pore size [8]. Furthermore, the utilized construction directing mediator for the production of triblock polymers are economical, harmless, and recyclable [6]. However, since the pore walls of SBA-15 were discovered to be amorphous, it lacks comparable acidity and necessitates acid centers unlike crystalline zeolite. [9]. In order to enhance the acid strength of SBA-15 for its implementations as a catalyst or support in acidic catalytic reactions, it is necessary to generate acid centers. Accordingly, for the creation of surface acidity, it is obligatory the inclusion of metallic ions, as Al, in the silica framework.

One of the main challenges is the requirement of a greatly acidic fabricated gel for the production of Al-SBA-15. In this particular case, the Al atoms exist as soluble components that are not remained within the SBA framework [10]. Aluminum may be added to SBA-15 via both post and direct artificial methods, according to the manufacturer. Aluminum oxides are generated within the pores and on the surface of materials fabricated through post-synthetic methods. The metal oxide blocks the pores moderately or totally, diminishing the surface characteristics [11–14]. Despite the simplicity of direct synthesis, its effectiveness is consistently limited owing to the low grafting of the supplied foreign atoms into the mesoporous structure, with only a small fraction being integrated. [15]. The production of Al-SBA-15 can be challenging, as aluminum must be grafted into the neutral silica framework without blocking the pores of the material. Several methods have been developed to overcome this challenge, including post-synthesis methods and direct synthesis methods[16–24]. Through the optimization of fabrication conditions, it becomes feasible to achieve high concentrations of Al3+ species and exceptional structural order in Al-SBA-15 materials.

The primary goals of this work are to explore the difficulties and progress made in the synthesis of mesoporous materials, specifically aluminum-containing silica, as catalyst in acidic catalytic reactions. The emphasis is placed on the integration of aluminum into the neutral SBA-15 matrix of to develop acid sites using the ionic-liquid approach. The study underscores the significance of developing mesoporous substances with high surface areas, evenly distributed pore sizes, and excellent chemical durability. Additionally, it highlights the potential implementations in catalysis.

2. Materials and Methods

2.1. Materials

Poly(ethylene oxide)-b-poly(propylene oxide)-b-poly(ethylene oxide) triblock copolymer Pluronic P123 (EO20PO70EO20, Mwt = 5800), tetraethylorthosilicate (TEOS, 98%), aluminum hexachloride (AlCl3 6H2O, 99%), hydrochloric acid (HCl, 37%), ethylenediamine (≥99%), (cumene (C6H5CH(CH3)2, 98%), acetic acid (CH3COOH, ≥ 99%), amyl alcohol (CH3(CH2)4OH, 99%), acetonitrile (CH3CN, 99%), n-butylamine (99.5%), acetic anhydride (≥98%), and anisole (99.7%) were acquired from Sigma- Aldrich Co., USA. and exploited as obtained. All the chemicals utilized as purchased without anu additional treatment.

2.2. Synthesis

2.2.1. Direct Alumination of SBA-15

To Aluminate SBA-15, two solutions have mixed together. The first solution was synthesized by introducing a certain quantity of amine to 10 ml of water, either 0.4 g of ethylenediamine or 1.25 g of triethylamine. This mixture was then treated with 10 ml of hydrochloric acid in a dropwise manner until it became neutral. Next, 1.65 g of aluminum chloride was introduced to the solution and agitated for two hours. Subsequently, a continuous stirring was applied to introduce 9.0 g of tetraethylorthosilicate (TEOS) into the solution, and this was followed by the introduction of 50 ml of hydrochloric acid (276). The second solution consisted of 8 g of Pluronic P123 dispersed in 100 ml of HCl solution, where the ratio of water to hydrochloric acid was 276. The blend was agitated for

 doi:10.20944/preprints202307.1258.v1

two hours until the Pluronic P123 had fully dissolved. Subsequently, the first solution was then mixed with a second solution under agitating for 24 hours. After the synthesis of aluminated SBA-15, the obtained material was treated hydrothermally for 24 hours at 100, 120, and 140 °C. The resulting white solid powder was separated, rinsed thoroughly with water, and then air-dried. The dried was then heated at 550 °C for a duration of 6 hours. This resulted in the formation of two different products: Al-SBA-15(Ex), where (E) denotes the use of ethylene diamine at x=100oC, 120oC and 140oC, and Al-SBA-15(Tx), where (T) represents the use of triethylamine at x=100oC, 120oC and 140°C.

2.3. Characterizations

The Fourier transform infrared spectroscopy was performed on pristine mesostructured materials and after the adsorption of pyridine using the Shimadzu IR Tracer-100 Fourier Transform infrared spectrometer (FTIR). The low-angle XRD patterns were acquired using the Shimadzu D/Max2500VB2+/Pc instrument with Cu Kα radiation (wavelength = 1.54056 Å). The measurements were taken within the 2θ range of 0.5 to 10°, with a step size of 0.01° and a step time of 10 seconds. The adsorption and desorption isotherms of nitrogen were obtained at 77 K using a NOVA 4200e instrument from Quanta chrome Instruments. A JEOL-2011, 200 kV instrument was utilized to acquire high-resolution transmission electron microscopy (HRTEM) images. In addition, the overall acidity of the solid samples was assessed using potentiometric titration. To conduct the titration, a mixture of the solid (0.05 g) and acetonitrile was stirred for 3 hours. Subsequently, titration was performed with 0.05 N 1-Aminobutane, in acetonitrile at a rate of 0.05 ml/min. The change in electrode potential was measured. NH3-TPD analysis was conducted utilizing a CHEMBET 3000 chemical absorber.

2.4. Catalytic performance assessment

2.4.1. Esterification

The acetic acid esterification was conducted utilizing 1 wt% of the catalyst. The process was performed in a 100 mL flask with a reflux, with the estimated amounts of butanol and acetic acid (in a 1:1 ratio). Two different temperatures, 80°C and 100°C, were employed. Throughout the esterification, samples of the blend were regularly collected and subjected to analysis utilizing gas chromatography (GC-Varian star CP-3800). The extent of conversion of acetic acid, represented as the percentage of acetic acid utilized, was determined by performing gas chromatographic analysis at different periods.

3. Results and Discussion

3.1. Materials characterization

The fabrication of mesoporous SBA-15 was achieved through hydrothermal methods under conditions of high acidity. The grafting of a significant quantity of aluminum ions into the SBA-15 structure under such conditions proved to be challenging. This difficulty may be because the elevated level of Al precursor solubility in an acidic environment, that limits its availability in its corresponding oxo species. As a result, the condensation process between the silicon species and Al atoms, which would facilitate the grafting of Al into the protonated mesoporous walls, is impeded by the strong repulsion forces between cationic silica and the positively charged Al-oxo components at smaller pH. Nonetheless, our prior investigation attempted to optimize the appropriate ratio of nH2O:nHCl. Based on our research, we discovered that when the ratio reaches 276, the pH level rises to approximately 2.4, surpassing the silica isoelectric point. As a result, the silica is a negatively charged, enabling it to interact with Al-oxo component, specifically Al(OH)2+. As a result of these findings, we determined that a ratio of 276 is the ideal proportion for preparing Al-SBA-15, as it enhances the quantity of Al3+ ions grafted into the SBA-15 walls. Table 1 lists the results of an elemental assessment conducted on the fabricated Al-SBA-15 using ICP, in the presence of either

Preprints (www.preprints.org) | NOT PEER-REVIEWED | Posted: 19 July 2023 doi:10.20944/preprints202307.1258.v1

ethylenediamine or triethyl amine ionic liquids, with a H2O: HCl ratio of 276. The element assessment showed that the Si/Al ratio varied depending on the kind of ionic liquid and the initial gel temperature. These findings suggest that using ethylenediamine or triethyl amine as ionic liquids in the presence of preformed Al-O-Si bonds is an effective method for preparing high Al3+ content Al-SBA-15 under acidic conditions at 120°C. However, the ICP data suggests that a higher amount of Al3+ is present in the materials prepared using triethyl amine ionic liquid.

Table 1. Texture properties of Al-SBA-15 materials prepared using ethylenediamine (E) and triethyl amine (T) at various temperature.

Sample	*n*Si/*n*Al	S_{BET}/ (m^2g^{-1})	V_P/ (cm^3/g)	D_P, ads/nm	*W (nm)*[a]
Al-SBA-15(E-100)	13	822	1.17	7.1	4.24
Al-SBA-15(T-100)	10	869	1.04	7.1	4.12
Al-SBA-15(E-120)	11	844	1.14	8.1	3.85
Al-SBA-15(T-120)	9	890	1.21	8.5	3.71
Al-SBA-15(E-140	31	319	1.12	8.7	3.15
Al-SBA-15(T-140)	36	333	1.01	8.5	3.26

Figure 1 presents the FT-IR spectra of different Al-SBA-15 structures that hydrothermally treated at different temperatures (100, 120, and 140 °C) and combined with various ionic liquids. The spectra reveal characteristic peaks that can be assigned to specific vibrational modes of the materials. The peak at approximately 1087 cm^{-1}. The presence of a shoulder around 1213 cm−1 in the observed spectra can be related to the Si-O-Si asymmetric mode. On the other hand, the symmetric stretching of these moieties is noted at approximately 810 and 554 cm^{-1}. The band at approximately 455 cm−1 was ascribed to the vibrational bending of either Al-O-Si or Si-O-Si bonds. The detection of a band at approximately 954 cm^{-1} suggests the existence of defective Si-OH moieties, which indicates the successful integration of Al3+ ions into the SBA-15 frameworks [25]. Furthermore, all the samples exhibit a broad characteristic peak between 3750-3100 cm^{-1}, which related to the excitation of H-bond (SiO–H) moieties [26]. This broad band is more prominent in the fabricated samples that hydrothermally treated at 120°C using either ethylenediamine or triethyl amine. This might be explained by the presence of hydroxyls in Al3+ ionic species that are in some extra-matrix of silica. The absorption of OH-Al species around 3700-3650 cm^{-1} coincides with the peak of H-bonded Si-OH, that are typically present in defective mesostructures. Moreover, there is a subtle absorption observed at approximately 3650 cm−1 in both Al-SBA-15(E-120) and Al-SBA-15(T-120), which can be attributed to the stretching vibration of OH groups in zeolite-type Si-OH-Al species present in the mesoporous aluminosilicate [27]. The increased concentration of Si-O-Al in the Al-SBA-15(E-120) and Al-SBA-15(T-120) samples can be attributed to the preparation conditions comprising the hydrothermal process at acidic pH. This acidic environment boosts the condensation of silanol moieties, leading to a higher presence of Si-O-Al bonds in the resulting materials.

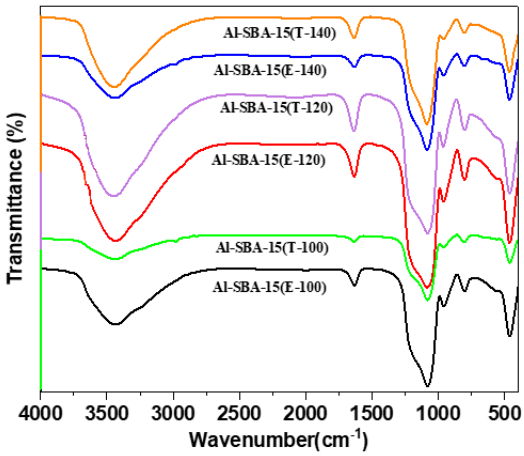

Preprints (www.preprints.org) | NOT PEER-REVIEWED | Posted: 19 July 2023 doi:10.20944/preprints202307.1258.v1

Figure 1. FTIR spectra of Al-SBA-15 materials fabricated with ethylenediamine and triethylamine and hydrothermally treated at varying temperatures (100, 120, and 140°C).

The XRD patterns of the Al-SBA-15 fabricated using various amine ionic liquids and hydrothermally treated at various temperatures are presented in Figure 2a. All materials display distinct XRD patterns that are specific to SBA-15 structures with hexagonal symmetry[10]. The presence of clearly distinguishable (100), (110), and (200) reflections indicates that the long-range mesoporous architecture remains intact even with the inclusion of aluminum.

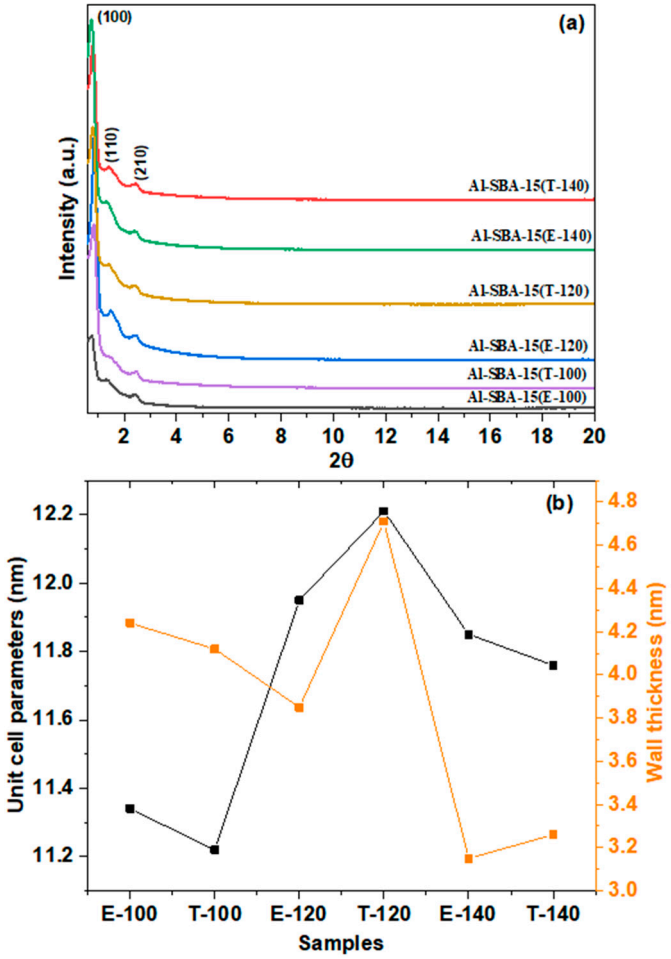

Figure 2. (a) Low-angle XRD patterns (b) Unite cell parameter and wall thickness of Al-SBA-15 materials fabricated with ethylenediamine and triethylamine and hydrothermally treated at varying temperatures (100, 120, and 140oC).

There were no more diffraction peaks corresponding to Al2O3 are noted in the Al-SBA-15 materials, suggesting that isolated Al2O3 clusters are not formed and the Al3+ ions are well-dispersed in the lattice without forming isolated Al2O3 clusters. The primary diffraction peaks in the Al-SBA-15(E-140 & T-140) samples are observed to shift towards smaller 2θ values. This change implies less structural contraction and lengthened Al-O bonds than Si-O bonds [28]. The hexagonal unit cell length (ao) was estimated based on the d-spacing of the (100) reflection and ranged from 11.34 to 12.21 nm (Figure 2b), with larger unit cell parameters observed for samples synthesized using diethylene amine and triethyl amine at 120 °C. This expansion of the lattice is attributed to the bigger Al3+ (53.5 pm) radius compared to Si4+ (40 pm). As a result, Si4+ is isomorphically replaced by Al3+ ions, and Al3+ ions are also grafted into the matrix or silica pore walls [29,30].

Figure 3 shows the 27Al nuclear magnetic resonance (NMR) spectra of Al-SBA-15(E-120) and Al-SBA-15(T-120) materials. The coordination of Al is notably affected by the choice of amine ionic liquids. The spectrum of Al-SBA-15(T-120) synthesized with triethyl amine at 120°C exhibits a single

Preprints (www.preprints.org) | NOT PEER-REVIEWED | Posted: 19 July 2023 doi:10.20944/preprints202307.1258.v1

strong peak at 61 ppm, demonstrating that the majority of aluminum is in tetrahedron-shaped coordinating sphere within the framework. On the other hand, Al-SBA-15(E-120) fabricated with ethylene diamine at 120°C shows two distinct bands at 1.7 and 55 ppm. The observed at 55 ppm is associated with aluminum ions in a tetrahedral coordinate, whereas the band at 1.7 ppm corresponds to octahedral aluminum, indicating the existence of aluminum extra-framework.

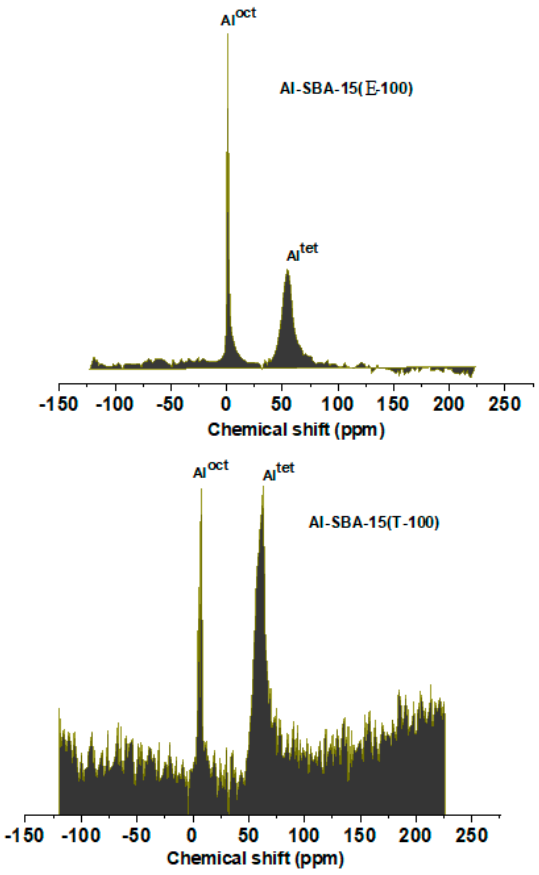

Figure 3. ^{27}Al NMR spectra of Al-SBA-15(E-120), and Al-SBA-15(T-120).

The study investigated the thermal stability of Al-SBA-15 materials fabricated using various amine ionic liquids. Figure 4a shows two temperature regions, each assigned to a weight loss event. During the temperature range of 30.5 to 95.6 °C, an initial event (I) took place, leading to a slight mass loss of 3.01%. This mass loss can be explained by the physical release of water and volatile components present within the porous structure. Between 95.6 and 660.7 °C, the second event (II) occurred, leading to a remarkable mass loss of 51.95%. This mass loss can be attributed to the elimination of ethylene diamine ionic liquid and P123 director. The system reached equilibrium at approximately 630 °C. Figure 4b depicts two distinct mass loss events. The initial weight-loss (I) took place within the temperature range of 31.3 to 72.1 °C, resulting in a mass loss of 3.73%. This mass loss can be attributed to the elimination of hydration water and the desorption of physiosorbed water within the porous structure. The second wight-loss (II) occurred between 72.1 and 710.2 °C, leading to a mass loss of 50.93%. This mass loss can be attributed to the removal of triethylamine ionic liquid and Pluronic P123.

Preprints (www.preprints.org) | NOT PEER-REVIEWED | Posted: 19 July 2023 doi:10.20944/preprints202307.1258.v1

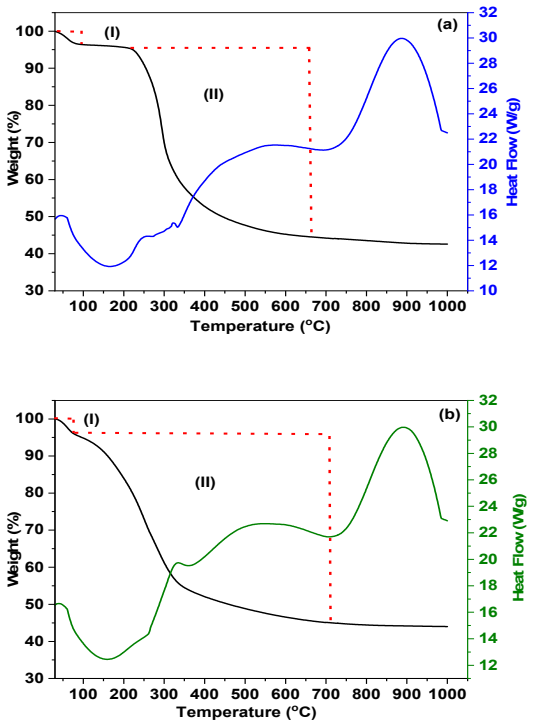

Figure 4. TGA profiles of (a) Al-SBA-15(E-120), and Al-SBA-15(T-120) materials.

Figure 5 presents transmission electron microscopy (TEM) images exhibiting the mesoporous structure of Al-SBA-15(E-120) and Al-SBA-15(T-120) materials at different magnifications. These images provide supporting evidence indicating that the grafting of Al3+ did not disturb the well-defined pore architecture present in the SBA-15 material. Furthermore, upon closer examination, the magnified images display a higher quantity of closely packed voids within the silica matrix fabricated via triethyl amine ionic liquid in comparison to those synthesized using ethylene diamine. This finding suggests that triethyl amine promotes the development of larger, well-organized pores.

Preprints (www.preprints.org) | NOT PEER-REVIEWED | Posted: 19 July 2023 doi:10.20944/preprints202307.1258.v1

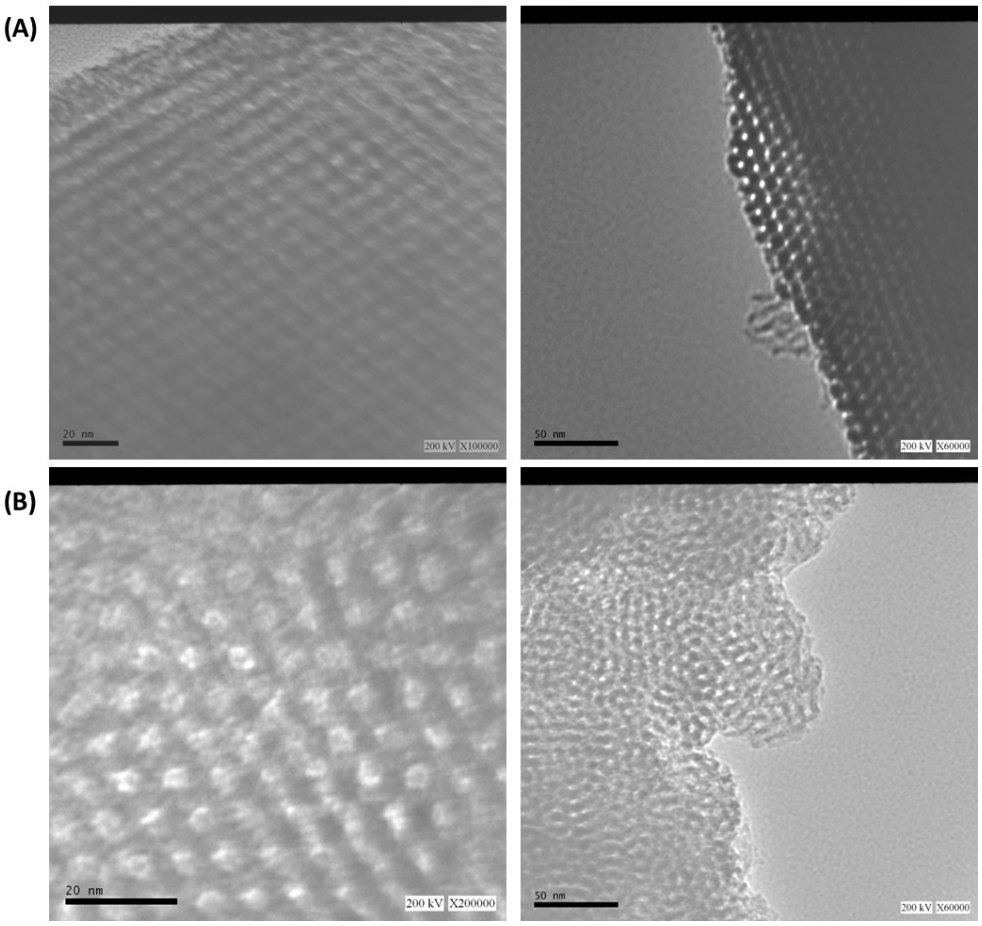

Figure 5. HRTEM images of (A) Al-SBA-15(E-120), and (B) Al-SBA-15(T-120) materials at different magnification.

Figure 6 illustrates the N_2-sorption isotherms for the Al-SBA-15 produced with various amine ionic liquids and hydrothermally treated at 100, 120, 140 °C. Table 1 provides a comprehensive overview of the textural properties exhibited by these materials. All the isotherms have an H1-type hysteresis loop and adhere to a standard type IV pattern, much like the SBA-15 isotherm. Nonetheless, the hysteresis loops observed for Al-SBA-15(E-140) and Al-SBA-15(T-140) materials lie between the H1 as well as H2 hysteresis loops, suggesting that their pore systems possess a somewhat lower degree of homogeneity compared to the samples subjected to hydrothermal treatment at 100°C and 120°C. All of the isotherms display a steep inflection when the relative pressure rises (P/Po > 0.5), that is consistent with capillary condensation of N2 inside homogenous mesopores. The diameter and limited distribution of mesopores are connected to the P/Po location and slopes of the inflection point (Figure 6b)[31]. The capillary condensation shifts to higher P/Po values with a raise in the hydrothermal temperature. This might be caused by a rise in director swelling when amine ionic solutions are present. The quantity of Al3+ ions within silica matrix significantly affects the surface area, specific pore volume, and pore size. Al-SBA-15 (E-100), (T-100), (E-120), (T-120), (E-140), and (T-140) have pores with diameters of roughly 7.1, 7.1, 8.1, 7.5, 8.7, and 8.5 nm, high BET surface areas of 822, 869, 844, 890, 319, and 333 m2 g−1, and pore volumes respectively, of 1.17, 1.04, 1.14, 1.21, 1.12, and 1.01 cm3 g−1. The reduced surface characteristics of Al-SBA-15(E-140) and Al-SBA-15(T-140) indicate lower Al2O3 distribution throughout the Al-SBA-15. Additionally, Al-SBA-15(E-140) and Al-SBA-15(T-140) showcase the smallest whole pore volume as a consequence of their diminished microporosity [32]. Generally, SBA-15 created using a great hydrothermal temperature (140 oC) comprise two interlaced subnetworks of pores. The development of a favorable pore architecture, that is frequently found within the walls of silica, is because the initial absorption of the ethylene oxide (EO) chains into the silica walls. The degree of interaction between EO and silica is significantly influenced by the hydrothermal temperature [33].

Preprints (www.preprints.org) | NOT PEER-REVIEWED | Posted: 19 July 2023 doi:10.20944/preprints202307.1258.v1

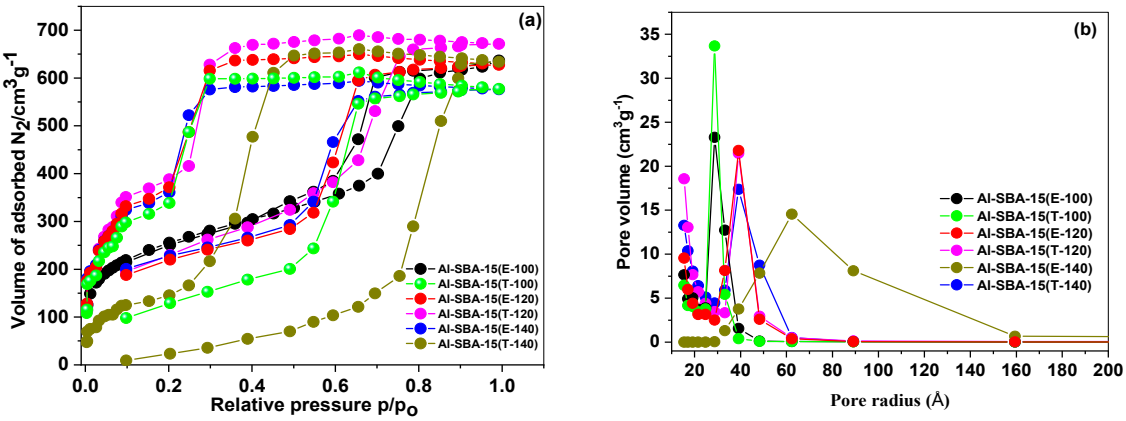

Figure 6. (a) Nitrogen adsorption isotherms and (b) pore size distribution of Al-SBA-15 materials fabricated with ethylenediamine and triethylamine and hydrothermally treated at varying temperatures (100, 120, and 140oC).

3.1.2. The characteristics of acid sites

The acidity of Al-SBA-15 samples was evaluated using three techniques, namely, potentiometric titration, NH3-TPD, and pyridine adsorption. Potentiometric titration was employed to examine the acid centers exist on the surfaces of the Al-SBA-15 catalysts, using n-butylamine. This technique allowed for an estimation of both the total number and relative strength of the acid centers in the materials. The magnitude of meq amine/g sample at the level of saturation provided the whole amount of acid centers, while the starting electrode potential (Ei) reflected the greatest acid sites strength. Based on the Ei values, the acid strength of the sites was classified into four categories: very weak sites (Ei < -100 mV), weak sites (-100 < Ei < 0 mV), strong sites (0 < Ei < 100 mV), and very strong sites (Ei > 100 mV) [3]. Table 2 summarizes the total quantity of acid sites and the initial potential (Ei) values for all samples, indicating that all samples possessed high surface acidity and acid strength. This enhancement in surface acidity and strength was credited with the homogenous distribution of Al3+ ions inside the pores of SBA-15 and on the upper surface. However, for the Al-SBA-15 prepared at 140 °C, the decline in acidity was due to the development of accumulated Al2O3.

Table 2. Acidic properties of Al-SBA-15 materials prepared using ethylenediamine (E) and triethyl amine (T) at various temperature.

Catalyst	E_i (mV)[a]	*Acid amount*/ (mmol n-butylamine)[a]	Total number of acid sites (mmol g^{-1})[b]	Number of acid sites (μmol g^{-1})[c]		B/L Ratio [c]
				Brönsted (B)	Lewis (L)	
Al-SBA-15(E-100)	99	0.22	0.897	18	11	1.64
Al-SBA-15(T-100)	111	0.31	0.934	21	14	1.50
Al-SBA-15(E-120)	120	0.43	1.012	33	18	1.83
Al-SBA-15(T-120)	130	0.55	1.134	43	21	2.05
Al-SBA-15(E-140	100	0.38	1.064	31	16	1.93
Al-SBA-15(T-140)	105	0.46	1.032	34	22	1.55

[a] Potentiometric titration. [b] NH_3-TPD. [c] Pyridine adsorption.

Preprints (www.preprints.org) | NOT PEER-REVIEWED | Posted: 19 July 2023 doi:10.20944/preprints202307.1258.v1

FT-IR spectroscopy with pyridine as a probe molecule was employed to investigate the distribution of Lewis (L) and Brønsted (B) acid sites in all Al-SBA-15 samples. The FT-IR spectra of pyridine adsorbed on the Al-SBA-15 samples are presented in Figure 7a. The results suggest that all the Aluminum incorporated samples possess both Lewis and Brønsted acidic centers, as demonstrated by the Infrared absorption peaks observed at approximately 1443 and 1544 cm^{-1}, respectively. Furthermore, the absorption peak at about 1491 cm−1 suggests the development of adjacent Lewis and Brønsted centers. The relative abundance of Brønsted and Lewis (B/L) acid centers ratio in each Al-SBA-15 sample was determined by examining the intensities of the corresponding FTIR bands, as presented in Table 2. An interesting observation is that Al-SBA-15(T-120) demonstrates a higher ratio of Brønsted/Lewis than the others, indicating a greater abundance of Brønsted acid sites. This implies that the Brønsted/Lewis's ratio rises alongside an increased presence of Brønsted acid sites in Al-SBA-15(T-120).

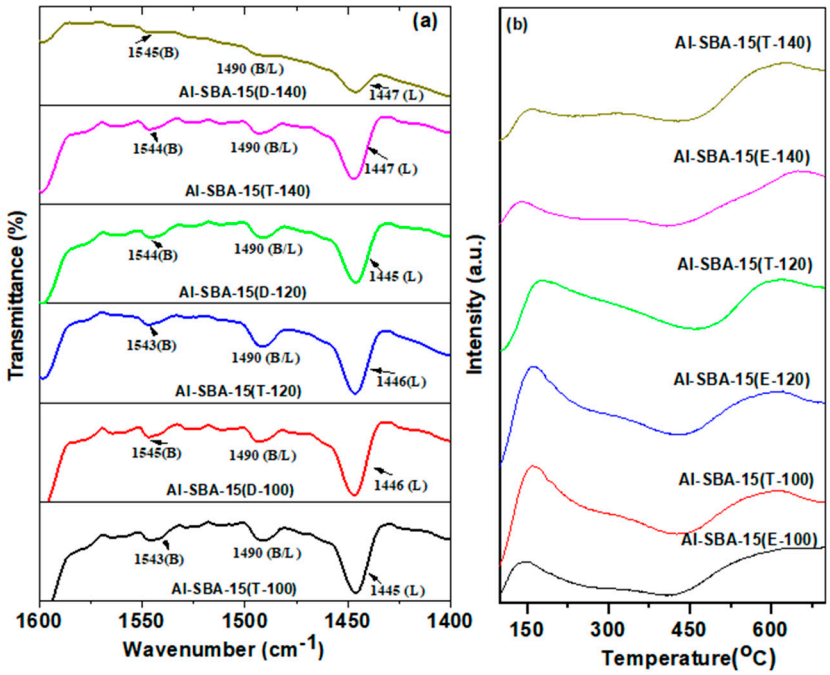

Figure 7. (a) Py-FTIR spectra, and (b) NH3-TPD profiles of Al-SBA-15 materials fabricated with ethylenediamine and triethylamine and hydrothermally treated at varying temperatures (100, 120, and 140°C).

The NH3-TPD profiles of various Al-SBA-15 samples (E-100, T-100, E-120, T-120, E-140, and T-140) are displayed in Figure 7b, and the total number of acid centers is provided in Table 2. The NH3-TPD plots reveal desorption peaks of NH3 between 100 and 550°C, indicating the presence of medium strength acidic sites. The observed peaks can be distinctly classified into three separate areas. The initial peak, observed at a lower temperature, is attributed to the presence of physiosorbed ammonia or NH3 molecules that are H-bonded to terminal silanol moieties.

The second peak, spanning the temperature range of 300 to 400°C, is associated with the adsorption of ammonia on aluminum (Al) within the matrix of the Al-SBA-15 samples. On the other hand, the presence of extra-framework (Al) is indicated by the third peak, observed at higher temperatures. Moreover, the total acidity of these materials can be ranked as follows: Al-SBA-15(T) > Al-SBA-15(E), as assessed by the whole acid centers estimated from NH3-TPD. The amorphous and thick pore wall in the mesoporous materials developed by ethylene diamine is responsible for the observed findings. In particular, the presence of Al atoms grafted within the thick walls of Al-SBA-15(E) makes them invisible to the probing molecule, thus complicating the evaluation of the acidic characteristics of the of prepared materials solely based on the coordination environment and

Preprints (www.preprints.org) | NOT PEER-REVIEWED | Posted: 19 July 2023 doi:10.20944/preprints202307.1258.v1

aluminum content. This highlights the challenge of assessing the acidic properties because the pore wall is thick and amorphous.

3.2. Catalytic performance

The catalytic efficiency of various Al-SBA-15 (E-100, T-100, E-120, T-120, E-140, and T-140) samples was investigated using the liquid phase esterification reaction as a laboratory probe. Both BAS (Brønsted acid sites) and LAS (Lewis's acid sites) were found to catalyze the esterification reaction [34]. It was also noted that Lewis's acid sites, particularly Mn+ ions with small coordination spheres, could be utilized [35]. Indeed, previous studies have predominantly emphasized the catalytic performance associated with Brønsted acid centers [10]. To facilitate a meaningful comparison between different samples, esterification reaction was chosen for the current research. The comparative findings of the catalytic efficiency can be illustrated in Figure 8. Among the examined catalysts, Al-SBA-15(T-120) demonstrated the greatest catalytic performance, resulting in a conversion rate of 38% and selectivity of approximately 100% towards butyl acetate. Figure 8 indicates that the efficiency of the catalysts can be ranked as follows: Al-SBA-15(E-120) < Al-SBA-15(T-120). The remarkable efficiency of Al-SBA-15(T-120) can be attributed to several factors, including its abundance of acidic centers, large surface area, and wide pore diameter. These characteristics facilitate the easy interact of reactants to the acidic protons, thereby enhancing the catalytic performance. On the other hand, the lower catalytic performance obtained for Al-SBA-15(E&T-140) in comparison to Al-SBA-15(E&T-100&120) can be credited with its declined surface area. The impact of esterification temperature (80°C and 100°C) and duration time is depicted in Figure 8. Generally, an increase in reaction temperature improves the catalytic performance. Specifically, for Al-SBA-15(T-120), the reaction proceeds rapidly, achieving approximately 32% and 38% conversion within 110 minutes at 80°C and 100°C, respectively. Importantly, the reaction exclusively yields butyl acetate as the product at all temperatures, demonstrating a 100% selectivity towards esterification.

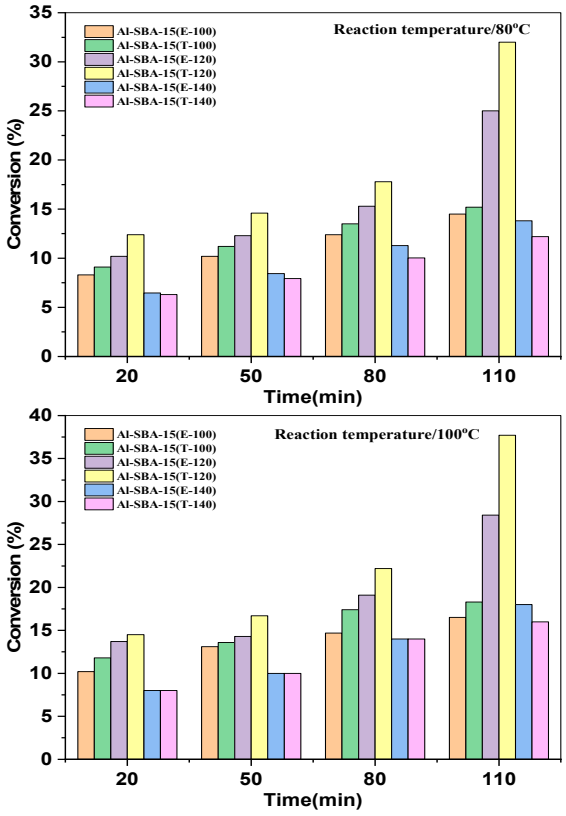

Figure 8. Catalytic performance of Al-SBA-15 materials fabricated with ethylenediamine and triethylamine and hydrothermally treated at varying temperatures (100, 120, and 140oC) on the esterification process at various temperatures and times.

5. Conclusions

An unprecedented achievement was made by successfully incorporating aluminum ions within the SBA-15 matrix using either ethylenediamine or triethyl amine ionic liquids. Various characterization techniques were employed to analyze the catalysts, demonstrating that the mesostructured of SBA-15 remained intact following the introduction of aluminum ions. However, there was a remarkable decline in the specific surface area and pore volume after grafting Al3+ ions. Additionally, a remarkable increase in surface acidity, including both Lewis and Bronsted acidity, was observed after the Al3+ ions grafting process. These catalysts exhibit tremendous potential for acid-catalyzed reactions and were effectively employed in an esterification reaction, resulting in a yield of over 38% at 100 °C using Al-SBA-15(T-120). These findings indicate that the fabricated catalysts show great potential and efficiency as acid catalysts. They can be regarded as suitable for industrial-scale applications.

Author Contributions: Conceptualization, M.S.A. and O.F.A..; methodology, M.S.A. and O.F.A..; software L.M.A., A.A., A.N.A., L.M.A; validation, H.M.H., M.S.A. and O.F.A.; formal analysis, L.M.A., A.A.; investigation, L.M.A., A.A., A.N.A., L.M.A; resources, O.F.A.; data curation, H.M.H., M.S.A. and O.F.A.; writing—original draft preparation, H.M.H., M.S.A. and O.F.A.; writing—review and editing., M.S.A. and O.F.A.; visualization, L.M.A., A.A.; H.M.H., M.S.A. and O.F.A.; supervision, O.F.A. All authors have read and agreed to the published version of the manuscript." Please turn to the CRediT taxonomy for the term explanation. Authorship must be limited to those who have contributed substantially to the work reported.

Funding: Please add: This research was funded by The Deputyship for Research & Innovation, Ministry Education in Saudi Arabia for Funding, grant number (Ifp-2022-39).

Acknowledgments: The Authors Extend Their Appreciation to The Deputyship for Research & Innovation, Ministry Education in Saudi Arabia for Funding This Research Work Through the Project Number (Ifp-2022-39).

Conflicts of Interest: The authors declare no conflict of interest.

References

1. M.R. Awual, Novel nanocomposite materials for efficient and selective mercury ions capturing from wastewater, Chem. Eng. J. 307 (2017) 456–465.
2. F.M. Mota, P. Eliášová, J. Jung, R. Ryoo, Mesoporous EU-1 zeolite as a highly active catalyst for ethylbenzene hydroisomerization, Catal. Sci. Technol. 6 (2016) 2735–2741.
3. S.K. Abd El Rahman, H.M.A. Hassan, M.S. El-Shall, Metal-organic frameworks with high tungstophosphoric acid loading as heterogeneous acid catalysts, Appl. Catal. A Gen. 487 (2014) 110–118.
4. M. Guisnet, J.-P. Gilson, Zeolites for cleaner technologies, Imperial College Press London, 2002.
5. A. Corma, Solid State Mat. Sci, Vol. 2 (1997) 63.
6. J.M.R. Gallo, C. Bisio, G. Gatti, L. Marchese, H.O. Pastore, Physicochemical characterization and surface acid properties of mesoporous [Al]-SBA-15 obtained by direct synthesis, Langmuir. 26 (2010) 5791–5800.
7. S. Chytil, W.R. Glomm, E.A. Blekkan, Characterization of Pt/SBA-15 prepared by the deposition–precipitation method, Catal. Today. 147 (2009) 217–223.
8. Y. Kang, X. Rao, P. Yuan, C. Wang, T. Wang, Y. Yue, Al-functionalized mesoporous SBA-15 with enhanced acidity for hydroisomerization of n-octane, Fuel Process. Technol. 215 (2021) 106765.
9. H.M.A. Hassan, M.A. Betiha, R.F.M. Elshaarawy, E.A. Ahmed, Facile tailoring of hierarchical mesoporous AlSBA-15 by ionic liquid and their applications in heterogeneous catalysis, J. Porous Mater. 25 (2018) 63–73.
10. M.A. Betiha, H.M.A. Hassan, A.M. Al-Sabagh, S.K. Abd El Rahman, E.A. Ahmed, Direct synthesis and the morphological control of highly ordered mesoporous AlSBA-15 using urea-tetrachloroaluminate as a novel aluminum source, J. Mater. Chem. 22 (2012) 17551–17559.
11. B. Dragoi, E. Dumitriu, C. Guimon, A. Auroux, Acidic and adsorptive properties of SBA-15 modified by aluminum incorporation, Microporous Mesoporous Mater. 121 (2009) 7–17.
12. P. Wu, T. Tatsumi, T. Komatsu, T. Yashima, Postsynthesis, characterization, and catalytic properties in alkene epoxidation of hydrothermally stable mesoporous Ti-SBA-15, Chem. Mater. 14 (2002) 1657–1664.

13. Z. Luan, M. Hartmann, D. Zhao, W. Zhou, L. Kevan, Alumination and ion exchange of mesoporous SBA-15 molecular sieves, Chem. Mater. 11 (1999) 1621–1627.
14. G. Lapisardi, F. Chiker, F. Launay, J.-P. Nogier, J.-L. Bonardet, A "one-pot" synthesis of adipic acid from cyclohexene under mild conditions with new bifunctional Ti-AlSBA mesostructured catalysts, Catal. Commun. 5 (2004) 277–281.
15. Y.G. Yue, A., Bonardet, J.-L., Melosh, N., and D'Espinose, J.-B, J. Fraissard, Chem. Commun. 19 (1999) 1967–1968.
16. L. Xiong, J. Shi, L. Zhang, M. Nogami, Facile one-step synthesis of highly ordered bimodal mesoporous phosphosilicate monoliths, J. Am. Chem. Soc. 129 (2007) 11878–11879.
17. N. Kemache, S. Hamoudi, J. Arul, K. Belkacemi, Activity and selectivity of nanostructured sulfur-doped Pd/SBA-15 catalyst for vegetable oil hardening, Ind. Eng. Chem. Res. 49 (2010) 971–979.
18. S.M. Rivera-Jiménez, S. Méndez-González, A. Hernández-Maldonado, Metal (M= Co2+, Ni2+, and Cu2+) grafted mesoporous SBA-15: Effect of transition metal incorporation and pH conditions on the adsorption of Naproxen from water, Microporous Mesoporous Mater. 132 (2010) 470–479.
19. J. Wang, Q. Liu, A simple method to directly synthesize Al-SBA-15 mesoporous materials with different Al contents, Solid State Commun. 148 (2008) 529–533.
20. J. Wang, Q. Liu, Q. Liu, Synthesis and characterization of Sn or Al-containing SBA-15 mesoporous materials without mineral acids added, Microporous Mesoporous Mater. 102 (2007) 51–57.
21. C.E. Garrett, K. Prasad, The art of meeting palladium specifications in active pharmaceutical ingredients produced by Pd-catalyzed reactions, Adv. Synth. Catal. 346 (2004) 889–900.
22. S. Wu, Y. Han, Y.-C. Zou, J.-W. Song, L. Zhao, Y. Di, S.-Z. Liu, F.-S. Xiao, Synthesis of heteroatom substituted SBA-15 by the "pH-adjusting" method, Chem. Mater. 16 (2004) 486–492.
23. Z.Y. Wu, H.J. Wang, T.T. Zhuang, L.B. Sun, Y.M. Wang, J.H. Zhu, Multiple Functionalization of Mesoporous Silica in One-Pot: Direct Synthesis of Aluminum-Containing Plugged SBA-15 from Aqueous Nitrate Solutions, Adv. Funct. Mater. 18 (2008) 82–94.
24. A. Vinu, V. Murugesan, W. Böhlmann, M. Hartmann, An optimized procedure for the synthesis of AlSBA-15 with large pore diameter and high aluminum content, J. Phys. Chem. B. 108 (2004) 11496–11505.
25. A. Zecchina, S. Bordiga, G. Spoto, L. Marchese, G. Petrini, G. Leofanti, M. Padovan, Silicalite characterization. 1. Structure, adsorptive capacity, and IR spectroscopy of the framework and hydroxyl modes, J. Phys. Chem. 96 (1992) 4985–4990.
26. K. Góra-Marek, M. Derewiński, P. Sarv, J. Datka, IR and NMR studies of mesoporous alumina and related aluminosilicates, Catal. Today. 101 (2005) 131–138.
27. F. Kleitz, F. Berube, R. Guillet-Nicolas, C.-M. Yang, M. Thommes, Probing adsorption, pore condensation, and hysteresis behavior of pure fluids in three-dimensional cubic mesoporous KIT-6 silica, J. Phys. Chem. C. 114 (2010) 9344–9355.
28. Y.-M. Liu, Y. Cao, N. Yi, W.-L. Feng, W.-L. Dai, S.-R. Yan, H.-Y. He, K.-N. Fan, Vanadium oxide supported on mesoporous SBA-15 as highly selective catalysts in the oxidative dehydrogenation of propane, J. Catal. 224 (2004) 417–428.
29. M. Selvaraj, D.-W. Park, C.S. Ha, Well ordered two-dimensional mesoporous CeSBA-15 synthesized with improved hydrothermal stability and catalytic activity, Microporous Mesoporous Mater. 138 (2011) 94–101.
30. T. Kudo, Y. Hisamitsu, K. Kihara, M. Mohamedi, I. Uchida, Electrochemical behaviour of Ni+ Al alloy as an alternative material for molten carbonate fuel cell cathodes, J. Appl. Electrochem. 32 (2002) 179–184.
31. K.S.W. Sing, Reporting physisorption data for gas/solid systems with special reference to the determination of surface area and porosity (Recommendations 1984), Pure Appl. Chem. 57 (1985) 603–619.
32. M. Imperor-Clerc, P. Davidson, A. Davidson, Existence of a microporous corona around the mesopores of silica-based SBA-15 materials templated by triblock copolymers, J. Am. Chem. Soc. 122 (2000) 11925–11933.
33. P.I. Ravikovitch, A. V Neimark, Characterization of micro-and mesoporosity in SBA-15 materials from adsorption data by the NLDFT method, J. Phys. Chem. B. 105 (2001) 6817–6823.
34. A.S. Khder, E.A. El-Sharkawy, S.A. El-Hakam, A.I. Ahmed, Surface characterization and catalytic activity of sulfated tin oxide catalyst, Catal. Commun. 9 (2008) 769–777.
35. S.L. Barbosa, M.J. Dabdoub, G.R. Hurtado, S.I. Klein, A.C.M. Baroni, C. Cunha, Solvent free esterification reactions using Lewis acids in solid phase catalysis, Appl. Catal. A Gen. 313 (2006) 146–150.
36. F.G. Bordwell, Equilibrium acidities in dimethyl sulfoxide solution, Acc. Chem. Res. 21 (1988) 456–463.
37. J. Han, G. Xu, B. Ding, J. Pan, H. Dou, D.R. MacFarlane, Porous nitrogen-doped hollow carbon spheres derived from polyaniline for high performance supercapacitors, J. Mater. Chem. A. 2 (2014) 5352–5357.
38. Y. Kubota, Y. Nishizaki, H. Ikeya, M. Saeki, T. Hida, S. Kawazu, M. Yoshida, H. Fujii, Y. Sugi, Organic–silicate hybrid catalysts based on various defined structures for Knoevenagel condensation, Microporous Mesoporous Mater. 70 (2004) 135–149.
39. X. Chen, M. Arruebo, K.L. Yeung, Flow-synthesis of mesoporous silicas and their use in the preparation of magnetic catalysts for Knoevenagel condensation reactions, Catal. Today. 204 (2013) 140–147.

 doi:10.20944/preprints202307.1258.v1